Topological insulator Bi₂Se₃ thin films grown on double-layer graphene by molecular beam epitaxy

Can-Li Song,[1,2] Yi-Lin Wang,[1] Ye-Ping Jiang,[1,2] Yi Zhang,[1] Cui-Zu Chang,[1,2] Lili Wang,[1] Ke He,[1] Xi Chen,[2] Jin-Feng Jia,[2] Yayu Wang,[2] Zhong Fang,[1] Xi Dai,[1] Xin-Cheng Xie,[1] Xiao-Liang Qi,[3] Shou-Cheng Zhang,[3] Qi-Kun Xue,[1,2,a)] and Xucun Ma[1]

[1]*Institute of Physics, Chinese Academy of Sciences, Beijing 100190, People's Republic of China*
[2]*Department of Physics, Tsinghua University, Beijing 100084, People's Republic of China*
[3]*Department of Physics, Stanford University, Stanford, California 94305-4045, USA*

Atomically flat thin films of topological insulator Bi₂Se₃ have been grown on double-layer graphene formed on 6H–SiC(0001) substrate by molecular beam epitaxy. By a combined study of reflection high energy electron diffraction and scanning tunneling microscopy, we identified the Se-rich condition and temperature criterion for layer-by-layer growth of epitaxial Bi₂Se₃ films. The as-grown films without doping exhibit a low defect density of $1.0 \pm 0.2 \times 10^{11}/cm^2$, and become a bulk insulator at a thickness of ten quintuple layers, as revealed by *in situ* angle resolved photoemission spectroscopy measurement. © *2010 American Institute of Physics.* [doi:10.1063/1.3494595]

Three dimensional (3D) topological insulators (TIs) such as Bi₂Se₃ and Bi₂Te₃ are characterized by a bulk energy gap of strong spin-orbit coupling origin and metallic surface states protected by time-reversal symmetry.[1–11] Without external doping, the Fermi level (E_F) of the materials resides in the bulk energy gap and thus only intersects the Dirac cone topological surface states,[1–6] which we call as "intrinsic" TI hereafter. A major experimental breakthrough in the emerging field of TIs is the material realization of high-quality single crystals by self-flux method.[2,3,5,12] However, as revealed by angle resolved photoemission spectroscopy (ARPES), the as-grown samples without doping are not a bulk insulator, rather, an n-type doped semiconductor,[2,3,5,12] presumably due to Se (Te) vacancies and antisite defects.[12–14] Further improvement in material quality via reducing/removing the Se (Te) vacancies is limited: it requires significant bulk diffusion of Se (Te) atoms in the quartz tube where the crystal forms, which is difficult because of the very volatile nature of Se or Te molecules compared to Bi. To reduce the unwanted electron carriers and move the E_F into the gap, a great number of carriers of opposite sign were introduced by extremely heavy doping with Sn atoms in Bi₂Te₃ (Ref. 5) and Ca atoms in Bi₂Se₃.[3,12]

In this work, we report molecular beam epitaxy (MBE) growth of high-quality Bi₂Se₃ thin films on double-layer graphene formed on the commercial 6H–SiC(0001) substrates.[15] The double-layer graphene has a similar layered structure to Bi₂Se₃ and is chemically inert due to the strong bonding of carbon atoms,[16] which turns out to greatly suppress interface reaction leading to atomically sharp interface between Bi₂Se₃ and graphene. We identify the layer-by-layer growth conditions of Bi₂Se₃ immediately on graphene by real-time reflection high energy electron diffraction (RHEED). *In situ* scanning tunneling microscope (STM) and ARPES measurements show that the as-grown films by our method are indeed a bulk insulator when the thickness is above 10 quintuple layers (QL). The resulting sharp interface

can be employed to study the interaction of the two distinct massless Dirac fermions in TI and graphene, respectively.

Our MBE growth and characterization of Bi₂Se₃ thin films were conducted in an ultrahigh vacuum (UHV) MBE-ARPES-STM combined system (Omicron) with a base pressure of 1×10^{-10} Torr. The double-layer graphene was prepared on a nitrogen-doped SiC(0001) substrate with a resistivity of ~ 0.1 Ω cm using the well-established recipe.[17] High purity Bi (99.999%) and Se (99.999%) were evaporated from standard Knudsen cells. ARPES spectra were collected at room temperature by a Gammadata Scienta SES-2002 analyzer with a HeI light source of 21.2 eV. We also used a low temperature STM system to characterize the as-grown films (Unisoku).[18] An MBE chamber is attached to the STM system and Bi₂Se₃ films were grown by using the same conditions mentioned above. STM images were taken at 4.8 K at a constant current of 0.1 nA with a polycrystalline W tip. The dI/dV mapping was acquired using a lock-in technique with a bias modulation of 10 mV at 987.5 Hz.[18]

The optimal conditions for layer-by-layer growth of bulk insulating Bi₂Se₃ films were established by a systematic investigation of the growth dynamics, surface morphology, and thickness-dependent electronic structure with RHEED, STM, and ARPES. Similar to those for GaAs (Ref. 19) and Bi₂Te₃,[6] the optimal growth can be achieved under Se-rich atmosphere (Se/Bi beam flux ratio $\theta \geq 10$) and $T_{Bi} > T_{substrate} > T_{Se}$ (T_{Bi}, $T_{substrate}$, and T_{Se} are the Bi-cell, substrate, and Se-cell temperatures, respectively). The former not only assures nucleation of the Bi₂Se₃ phase than other phases, according to the phase diagram[20] but also minimizes the formation of Se vacancy, which is difficult in self-flux method.[2,3,5,12] Under Se-rich condition, there always exist extra Se molecules on the growing front. However, these molecules cannot be incorporated into the film and will desorb since $T_{substrate} > T_{Se}$. The optimal growth is demonstrated in Fig. 1. The film shown in this figure was grown at $\theta = 11$, $T_{Bi} = 550$ °C, $T_{Se} = 136$ °C, $T_{substrate} = 220$ °C and has a nominal thickness of 26 QL. The characteristic RHEED intensity oscillation recorded during film deposition indicates
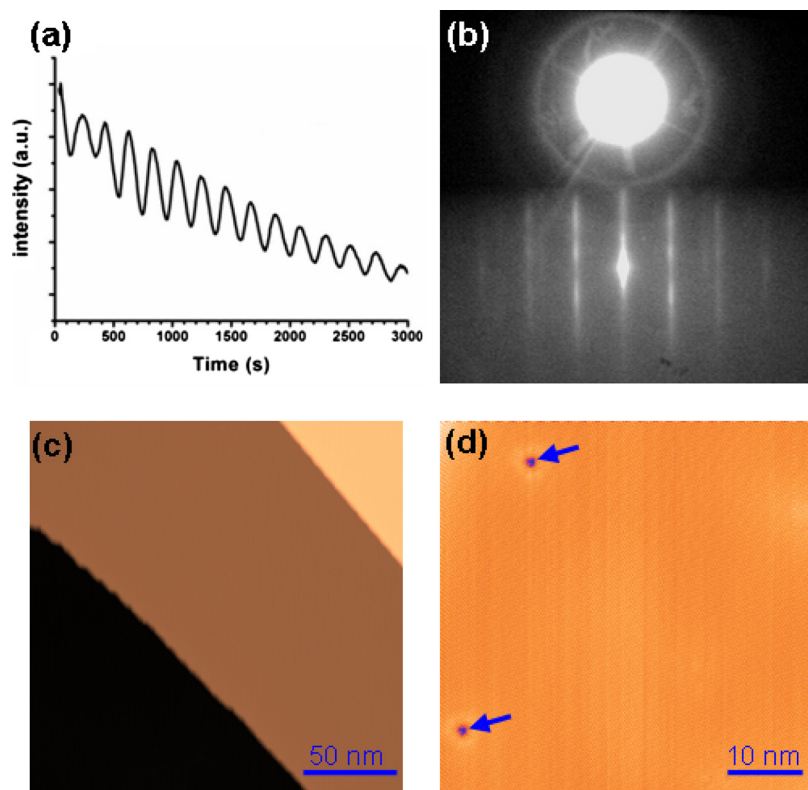
FIG. 1. (Color online) (a) RHEED intensity of the (0, 0) diffraction vs growth time. (b) RHEED pattern along Γ-K direction and (c) STM image of the 26 QL Bi$_2$Se$_3$ film acquired at a sample bias (V_s) of 1.0 V. (d) STM image (V_s = 10 mV) showing the Se vacancies (arrows).

an ideal layer-by-layer growth [Fig. 1(a)], where each circle of the oscillations corresponds to deposition of 1 QL of Bi$_2$Se$_3$. Therefore, the growth rate can be precisely measured, which is ~0.3 QL/min in this case. The atomically flat nature of the film is first evidenced by the sharp 1×1 RHEED pattern in Fig. 1(b) and further demonstrated by the STM image in Fig. 1(c). As expected, the steps seen in the STM image have a height of 0.95 nm, exactly the QL unit cell size of Bi$_2$Se$_3$ along the c axis.[21] The Se-rich condition results in very few defects in the as-grown samples. A typical STM image of the film is shown in Fig. 1(d). Only two defects can be found in an area of 50×50 nm^2. The dominant defects are Se vacancies [the dark depressions in Fig. 1(d)], which can be identified by their registry with respect to the topmost Se lattice. The areal defect density in this sample is ~1.0±0.2×10^{11}/cm^2, which is much lower than that on the cleaved samples.[12] Further investigation indicates fewer vacancy defects if higher Se/Bi flux ratio is used.

The electronic structure of the film is studied by ARPES and shown in Fig. 2(a). The Dirac cone (the dashed red lines) can be clearly seen, and the Dirac point is located at 130 meV below E_F. While the position of the Dirac point can change (several tens of millielectron volts) with film thickness, what is important here is that the intense electronic pocket from the bulk conduction band observed in the cleaved crystals[2,3,12] does not appear, suggesting that the film at this thickness is already a bulk insulator. Given the conditions we used, it is found that the minimum thickness for the film being an intrinsic TI is 11 QL. The details of this result has been discussed elsewhere.[4]

We also tried another substrate Si(111)-7×7. To avoid possible formation of SiSe$_2$ and other selenides at the interface,[22] the Bi-terminated √3×√3 structure was first grown.[21] In spite of it, the morphology of the Bi$_2$Se$_3$ films on the Bi-terminated √3×√3 surface, especially in the very

thinner regime, is ill-defined. Moreover, the films suffer from stronger electron-doping, which can be seen by a comparison of the ARPES data on both substrates [Fig. 2(b)]. Clearly, the Bi$_2$Se$_3$(111) films on graphene show much quicker development to the bulk insulating state than those on the √3×√3-Bi/Si(111) substrate, suggesting more defects and poorer film quality in the latter case. The critical thickness for intrinsic TIs on the Bi-terminated Si(111) surface is as high as 24 QL.

Now we discuss the role of the double-layer graphene. In a heteroepitaxial growth, the interface plays very critical roles in growth mode, strain relaxation, and formation of defects such as misfit and screw dislocations. The situation becomes even more severe when a film is being deposited on a substrate of different material, for example, Bi$_2$Se$_3$ on Si in which strong surface selenization by Se molecules may occur. By using inert graphene substrate, we found that not only is the interface reaction completely suppressed but also could the strain relaxation be complete at the very first epi-
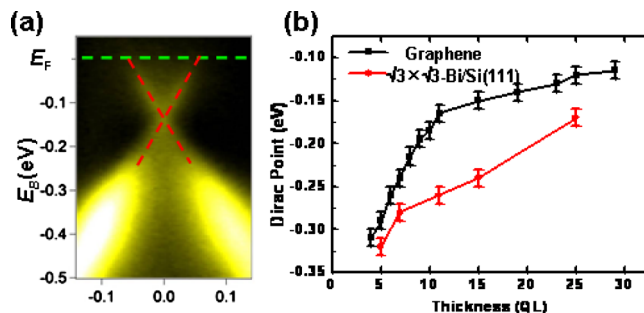
FIG. 2. (Color online) (a) ARPES intensity map of the 26 QL film along the Γ-K direction. The dotted line indicates the Fermi level, and the topological surface states, respectively. (b) Thickness-dependent surface Dirac point of Bi$_2$Se$_3$ films on graphene and Si substrates.
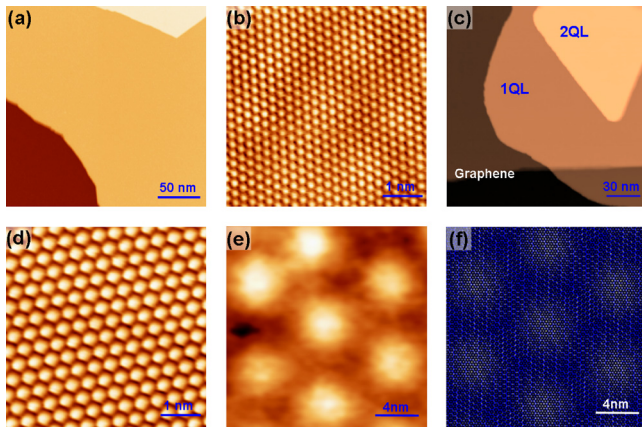
FIG. 3. (Color online) (a) Large scale ($V_s = 4.0$ V) and (b) atomic resolution STM images ($V_s = 10$ meV) of double-layer graphene on SiC(0001) substrate. (c) STM image ($V_s = 1.0$ V) recorded after deposition of 1.5 QL Bi_2Se_3 on graphene. (d) High-resolution STM image ($V_s = 10$ meV) of 1 QL Bi_2Se_3 film. The bright spot corresponds to a topmost surface Se atom. (e) dI/dV mapping of 1 QL Bi_2Se_3 film at $V_s = -0.35$ V, revealing a Moiré pattern with a period of 7.10 nm. (f) Simulated Moiré pattern by assuming a fully relaxed Bi_2Se_3 on graphene.

taxial layer of Bi_2Se_3, which does not necessarily induce any dislocations expected from the large lattice mismatch between graphene and Bi_2Se_3. Figures 3(a) and 3(b) show the morphology and hexagonal atomic lattice of the graphene, respectively, prepared on 6H–SiC(0001). After deposition of Bi_2Se_3 for 5 min (corresponding to a nominal thickness of ~ 1.5 QL), single crystalline Bi_2Se_3 film is formed [Fig. 3(c)]. At this stage, both 1 and 2 QL islands are observed, implying an incomplete wetting of the graphene surface. From the atomically resolved STM image of the 1 QL Bi_2Se_3 film in Fig. 3(d), we know that $Bi_2Se_3(111)$-1×1 surface is formed. The surface lattice constant measured with respect to the exposed graphene is 0.41 ± 0.01 nm, consistent with that (0.414 nm) of the bulk $Bi_2Se_3(111)$ surface. The observation reveals that the strain is already fully relaxed even at the first QL. According to Figs. 3(b) and 3(d), the close-packed direction of the Se atoms is rotated by 28° with respect to that of the graphene. This leads to a well-defined Morié pattern with a period of ~ 7.10 nm, as observed from dI/dV mapping at -0.35 V [Fig. 3(e)]. Assuming that the $Bi_2Se_3(111)$ film is fully relaxed, a simple simulation [Fig. 3(f)] indicates that, to form the Morié pattern in Fig. 3(e), the in-plane close-packed direction of the $Bi_2Se_3(111)$ film should be rotated by 29°, which is very close to the experimental value. It further supports a fully relaxed Bi_2Se_3 film at 1 QL. Evidently, no interface reaction occurs and the Bi_2Se_3/graphene interface is atomically sharp.

In summary, we have shown that graphene can serve a superb substrate for growing high quality Bi_2Se_3 films. Under the growth criteria established in this study, intrinsic TI films can be easily obtained when the thickness is above 10 QL. We emphasize that the growth conditions presented here can be applied to growth of other V-VI topological thin films and their heterostructures by standard MBE technique.

[1] H. J. Zhang, C. X. Liu, X. L. Qi, X. Dai, Z. Fang, and S. C. Zhang, Nat. Phys. **5**, 438 (2009).
[2] Y. Xia, D. Qian, D. Hsieh, L. Wray, A. Pal, H. Lin, A. Bansil, D. Grauer, Y. S. Hor, R. J. Cava, and M. Z. Hasan, Nat. Phys. **5**, 398 (2009).
[3] D. Hsieh, Y. Xia, D. Qian, L. Wray, J. H. Dil, F. Meier, J. Osterwalder, L. Patthey, J. G. Checkelsky, N. P. Ong, A. V. Fedorov, H. Lin, A. Bansil, D. Grauer, Y. S. Cava, and M. Z. Hasan, Nature (London) **460**, 1101 (2009).
[4] Y. Zhang, K. He, C. Z. Chang, C. L. Song, L. L. Wang, X. Chen, J. J. Jia, Z. Fang, X. Dai, W. Y. Shan, S. Q. Shen, Q. Niu, X. L. Qi, S. C. Zhang, X. C. Ma, and Q. K. Xue, Nat. Phys. **6**, 584 (2010).
[5] Y. L. Chen, J. G. Analytis, J. H. Chu, Z. K. Liu, S. K. Mo, X. L. Qi, H. J. Zhang, D. H. Lu, X. Dai, Z. Fang, S. C. Zhang, I. R. Fisher, Z. Hussain, and Z. X. Shen, Science **325**, 178 (2009).
[6] Y. Y. Li, G. Wang, X. G. Zhu, M. H. Liu, C. Ye, X. Chen, Y. Y. Wang, K. He, L. L. Wang, X. C. Ma, H. J. Zhang, X. Dai, Z. Fang, X. C. Xie, Y. Liu, X. Q. Qi, J. F. Jia, S. C. Zhang, and Q. K. Xue, Adv. Mater. **22**, 4002 (2010).
[7] P. Roushan, J. Seo, C. V. Parker, Y. S. Hor, D. Hsieh, D. Qian, A. Richardella, M. Z. Hasan, R. J. Cava, and A. Yazdani, Nature (London) **460**, 1106 (2009).
[8] T. Zhang, P. Cheng, X. Chen, J. J. Jia, X. C. Ma, K. He, L. L. Wang, H. J. Zhang, X. Dai, Z. Fang, X. C. Xie, and Q. K. Xue, Phys. Rev. Lett. **103**, 266803 (2009).
[9] X. L. Qi and S. C. Zhang, Phys. Today **63**(1), 33 (2010).
[10] J. E. Moore, Nature (London) **464**, 194 (2010).
[11] M. Z. Hasan and C. L. Kane, Rev. Mod. Phys. (in press).
[12] Y. S. Hor, A. Richardella, P. Roushan, Y. Xia, J. G. Checkelsky, A. Yazdani, M. Z. Hasan, N. P. Ong, and R. J. Cava, Phys. Rev. B **79**, 195208 (2009).
[13] S. Urazhdin, D. Bilc, S. H. Tessmer, and S. D. Mahanti, Phys. Rev. B **66**, 161306(R) (2002).
[14] S. Urazhdin, D. Bilc, S. D. Mahanti, and S. H. Tessmer, Phys. Rev. B **69**, 085313 (2004).
[15] W. H. Dang, H. L. Peng, H. Li, P. Wang, and Z. F. Liu, Nano Lett. **10**, 2870 (2010).
[16] A. K. Geim and K. S. Novoselov, Nature Mater. **6**, 183 (2007).
[17] J. Hass, W. A. D. Heer, and E. H. Conrad, J. Phys.: Condens. Matter **20**, 323202 (2008).
[18] X.-C. Ma, P. Jiang, Y. Qi, J.-F. Jia, Y. Yang, W.-H. Duan, W.-X. Li, X. Bao, S. B. Zhang, and Q.-K. Xue, Proc. Natl. Acad. Sci. U.S.A. **104**, 9204 (2007).
[19] Q. K. Xue, T. Hashizume, and T. Sakurai, Prog. Surf. Sci. **56**, 1 (1997).
[20] H. Okamoto and L. E. Tanner, *Bi-Se (Bismuth-Selenium) Phase Diagram* (ASM, Metals Park, OH, 1986).
[21] G. H. Zhang, H. J. Qin, J. Teng, J. D. Guo, Q. L. Guo, X. Dai, Z. Fang, and K. H. Wu, Appl. Phys. Lett. **95**, 053114 (2009).
[22] R. D. Bringans and M. A. Olmstead, Phys. Rev. B **39**, 12985 (1989).